Probable cross-corridor transmission of SARS-CoV-2 due to cross airflows and its control

Pan Cheng [a], Wenzhao Chen [a], Shenglan Xiao [b], Fan Xue [c], Qun Wang [a], Pak Wai Chan [d], Ruoyu You [f], Zhang Lin [e], Jianlei Niu [f], Yuguo Li [a,g,*]

[a] Department of Mechanical Engineering, The University of Hong Kong, Hong Kong SAR, China
[b] School of Public Health (Shenzhen), Sun Yat-sen University, Shenzhen, China
[c] Department of Real Estate and Construction, The University of Hong Kong, Hong Kong SAR, China
[d] Hong Kong Observatory, Kowloon, Hong Kong SAR, China
[e] Division of Building Science and Technology, City University of Hong Kong, Hong Kong SAR, China
[f] Department of Building Environment and Energy Engineering, The Hong Kong Polytechnic University, Hong Kong SAR, China
[g] School of Public Health, The University of Hong Kong, Hong Kong SAR, China

ARTICLE INFO

ABSTRACT

A COVID-19 outbreak occurred in May 2020 in a public housing building in Hong Kong – Luk Chuen House, located in Lek Yuen Estate. The horizontal cluster linked to the index case' flat (flat 812) remains to be explained. Computational fluid dynamics simulations were conducted to obtain the wind-pressure coefficients of each external opening on the eighth floor of the building. The data were then used in a multi-zone airflow model to estimate the airflow rate and aerosol concentration in the flats and corridors on that floor. Apart from flat 812 and corridors, the virus-laden aerosol concentrations in flats 811, 813, 815, 817 and 819 (opposite to flat 812, across the corridor) were the highest on the eighth floor. When the doors of flats 813 and 817 were opened by 20%, the hourly-averaged aerosol concentrations in these two flats were at least four times as high as those in flats 811, 815 and 819 during the index case's home hours or the suspected exposure period of secondary cases. Thus, the flats across the corridor that were immediately downstream from flat 812 were at the highest exposure risk under a prevailing easterly wind, especially when their doors or windows that connected to the corridor were open. Given that the floorplan and dimension of Luk Chuen House are similar to those of many hotels, our findings provide a probable explanation for COVID-19 outbreaks in quarantine hotels. Positive pressure and sufficient ventilation in the corridor would help to minimise such cross-corridor infections.

1. Introduction

Several Coronavirus Disease 2019 (COVID-19) outbreaks involving probable airborne transmission of severe respiratory syndrome coronavirus 2 (SARS-CoV-2) in poorly ventilated spaces have been documented and investigated [1–4]. The airborne transmission of SARS-CoV-2 has also been recognised by the World Health Organization since July 2020 [5].

Theoretically, if airborne transmission occurs within poorly ventilated indoor spaces, then transmission between two or more directly connected and poorly ventilated small indoor spaces is also possible. In this case, direct connection refers to the direct airflow between separated spaces without significant filtration and deposition during air exchange. Transmission between guest rooms and the corridor or between guest rooms sharing the same corridor has been reported in quarantine hotels in many countries such as Australia [6], Canada [7], New Zealand [8], China and the UK [9], and Hong Kong [1,2,10]. By June 15, 2021 Australia experienced 22 COVID-19 outbreaks in quarantine hotels, while New Zealand reported 10 [11]. An outbreak at Rydges Hotel and another at Stamford Plaza Hotel in Melbourne led to the second wave of infections in Victoria, Australia, with 99% of the over 19,800 cases linked to infections at these two hotels. This wave of infections resulted in more than 800 deaths and a lockdown of the state that lasted 112 days [12]. A lockdown in Victoria may cost AU$1 billion

a week [8]. In Australia and New Zealand, an estimated 5.0 quarantine system failures per 100,000 travellers and 6.1 quarantine system failures per 1000 positive cases of SARS-CoV-2 were estimated [8]. In Hong Kong, one guest in a quarantine hotel that had ventilation that was 'not up to standard' caught the virus from two people who were staying in the room that was directly opposite across the corridor [13]. Environmental samples taken from the rooms tested positive for the virus [14], although fomite transmission was deemed to be unlikely [15].

The COVID-19 pandemic has seen the emergence of 'quarantine hotels', venues specifically dedicated to isolate newly arrived travellers and contain the spread of the virus. Guests of quarantine hotels are typically confined to their rooms for fixed periods (e.g., 14 days or 21 days). During this period, the guests are strictly required to stay in their rooms; they are only allowed to open their doors occasionally to receive deliveries of food and other essential items, as well as provide samples for swab tests. In some countries, no other people are allowed to enter guests' rooms throughout the entire duration of the stay. As there is no close contact or sharing of items between guests or between guests and hotel workers, an occurrence of transmission would indicate that transmission is airborne.

With the exception of facilities that were specially built for quarantine recently [16], most quarantine hotels were neither designed nor constructed for quarantine purposes. Thus, there is an urgent need to understand the conditions under which the transmission of infections occur and to develop intervention strategies.

As with investigations of other airborne outbreaks, quantifying the airflow between rooms and the ventilation rate within rooms is important for revealing the virus-laden aerosol transport and possibility of airborne transmission. However, there is currently limited access to quarantine hotels to conduct such investigations due to the continued use of the facilities for quarantine during the ongoing pandemic, even after outbreaks are identified. Given that COVID-19 outbreaks have been reported in ordinary hotels (e.g., Ref. [17], it is unsurprising that SARS-CoV-2 can also be transmitted between guests and workers in quarantine hotels. In 2003, a major outbreak of SARS occurred in a hotel in Hong Kong [18]. It resulted in 13 cases of infection, 9 of whom (including the index case) stayed on the ninth floor of the hotel. The infected international travellers travelled elsewhere and initiated outbreaks in numerous other countries, including Singapore and Canada [18].

In June 2020, we carried out field measurements of the dispersion of tracer gas in Luk Chuen House in Hong Kong [19]. A COVID-19 outbreak had occurred here at the end of May 2020, and a cross-corridor virus transmission was suspected (Fig. 1a). Built in 1975, Luk Chuen House is a multistorey public housing building with a floorplan similar to those of typical multistorey hotels, in which separate flats (or rooms in the case of a hotel) are located along both sides of a long corridor (Fig. 1b, [20]. The outbreak included two spatial clusters [19]: a horizontal cluster on the eighth floor, including flat 812 where the index case lived and flats 813 and 817 where secondary infections occurred (Fig. 1a); and a vertical cluster connected by the building's shared drainage system (including flats 710, 810, 1012 and 1112). Wang et al. [19] conducted a detailed investigation of the role of the unusual two-stack drainage system that connected the flats in spreading the virus in the vertical cluster. The potential role of airflow between flats in facilitating cross-corridor virus transmission in the horizontal cluster was discussed in this study.

Here we present a focused and detailed investigation of the horizontal cluster in the COVID-19 outbreak in Luk Chuen House. Specifically, using multi-zone modelling of airflows driven by winds and the buoyancy in the building, we explain how airborne transmission contributed to the outbreak. We discuss the implications of the findings for virus transmission between guest rooms in quarantine hotels that have a similar floorplan to that of Luk Chuen House, although the corridors are naturally ventilated in Luk Chuen House and mechanically ventilated in most quarantine hotels as discussed later. To achieve the above objectives, we estimate the hourly variation in aerosol concentrations in flats and the corridor on the eighth floor of Luk Chuen House during the suspected exposure period. We used the relevant field measurements and data from the literature to validate the modelling study.
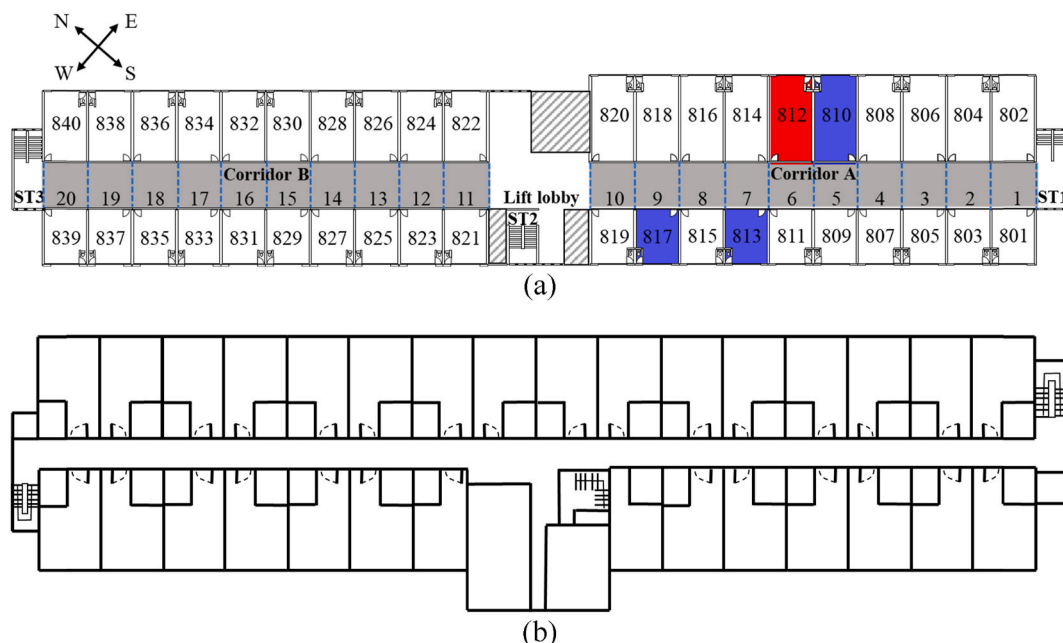
Fig. 1. Floorplan of the eighth floor of Luk Chuen House showing the flats with infected cases, and a typical floorplan of a hotel. (a) Layout of the eighth floor of Luk Chuen House. Spaces with line shading – that is, the lifts, refuse room and switch room – were not included in the airflow analysis. There are 40 flats (801–840) on the eighth floor, three stairwells (ST1, ST2 and ST3), two corridors (Corridor A and Corridor B, and each corridor is divided into 10 corridor zones), and one lift lobby. Flat 812, where the index case lived, is shown in red, while flats 810, 813 and 817 where secondary infections occurred are shown in blue. (b) A typical floorplan of a hotel, re-drawn based on the hotel depicted in Bahadori-Jahromi et al. [20]. Both layouts are not drawn to scale.

2. Methods

2.1. The outbreak

The index patient was a 34-year-old female nightshift worker who worked in a warehouse where fruit and vegetables imported from a European country were labelled. She developed a cough and fatigue on 22 May 2020 and was later hospitalised on 30 May 2020. Through contact tracing, two co-workers in the warehouse with earlier symptom onset – on 25 and 27 April 2020 – were identified. The index case lived in flat 812 of Luk Chuen House (Fig. 1a). Between 31 May and 13 June 2020, SARS-CoV-2 infections were confirmed in nine residents living in Luk Chuen House. Among the flats with infected residents, flat 812 (where the husband and sister of the index case were infected), flats 813 (one senior female infected), and flat 817 (one senior female infected) formed a horizontal cluster.

We obtained the hourly weather data recorded at Shatin station from 21 May to 24 May 2020 from the Hong Kong Observatory (Fig. 2). The possible exposure period was suspected to begin from 00:00 on 22 May to 24:00 on 24 May 2020, when the index case was believed to have a peak viral load (i.e., within 2 days before and after the onset of her symptoms). Due to unfavourable background wind conditions, the date 21 May was excluded from the study period. During the suspected 72-h exposure period from 22 May to 24 May 2020, the wind direction fluctuated between a northerly and south-westerly direction. Wind angle in the vertical axis of Fig. 2 is the angle between wind incoming direction and the north direction, which ranges from 0 to 360°. When the angle is within the range of 22.5–67.5°, the wind direction is said to be northeasterly. Similarly, 67.5–112.5°, easterly; and so on.

The outbreak occurred during a time when there were no other locally transmitted cases in Hong Kong [19]. The building has 15 storeys, with residential flats located on 2F–15F. Each floor contains 40 flats, with 20 flats lining each side; this corresponds to 40 columns of flats in the building. A flat is defined here as a residential unit and referred to as 'flat ##&&', in which '##' refers to the floor level, and '&&' refers to flat number. For instance, flat 0812 – or its shortened version 812 – refers to the twelfth flat (i.e., flat number 12) on the eighth floor. Each column of flats is referred to as '-&& flats'; for instance, '-12 flats' refers to the column of flats sharing the flat number 12 that are aligned vertically across all floors. Columns of flats that are adjacent to

one another are connected by a shared two-stack drainage pipe. For example, the −10 flats and the −12 flats, which are adjacent to each other, share a two-stack drainage pipe; this was found to be the likely cause of the vertical spread of the virus from flat 812 (and possibly flat 810) to flats 710, 1012 and 1112 [19]. Each of the two corridors is divided into 10 corridor zones, i.e., corridor A divided into corridor zones 1–10 and B into 11–20. Thereafter, each corridor zone will be referred to by their zone number. For example, corridor zone 10 is the corridor zone next to the lift lobby and connects flats 819 and 820.

2.2. Computer modelling

We first conducted a CFD simulation to investigate the patterns of airflow around the building under wind directions that possibly occurred during the suspected exposure period. The CFD simulation encompassed a domain that was 2 km long (streamwise direction), 1 km wide and approximately 500 m high; this included Luk Chuen House and its 126 buildings in the surrounding area (Fig. 3a). The commercial software ANSYS Fluent was used for CFD simulations. A pressure-based solver was used, and only a steady-state solution was obtained. The thermal buoyancy effect on wind flows was not considered, and the realisable k-epsilon model with standard wall functions was used to model turbulence. The second-order upwind scheme were used for gradient, pressure, momentum, turbulent kinetic energy, and turbulent dissipation rate discretisation.

The inlet velocity is an exponential function of height (Hsu et al., 1994).

$$U(z) = U_{free} \bullet \left(\frac{z}{40}\right)^{0.11} \tag{1}$$

when z is less than or equal to 40 m;

$$U(z) = U_{free} \tag{2}$$

when z is larger than 40 m, where U_{free} is the average wind speed during the investigation period multiplied by 1.11. An outflow condition was applied on the downwind boundary, opposite to the inlet boundary. The top and sides of the computation domain were symmetrical.

All buildings were assumed to have sealed walls; this meant that the cross ventilation inside each building was not included in the CFD modelling. In accordance with the wind directions detected during
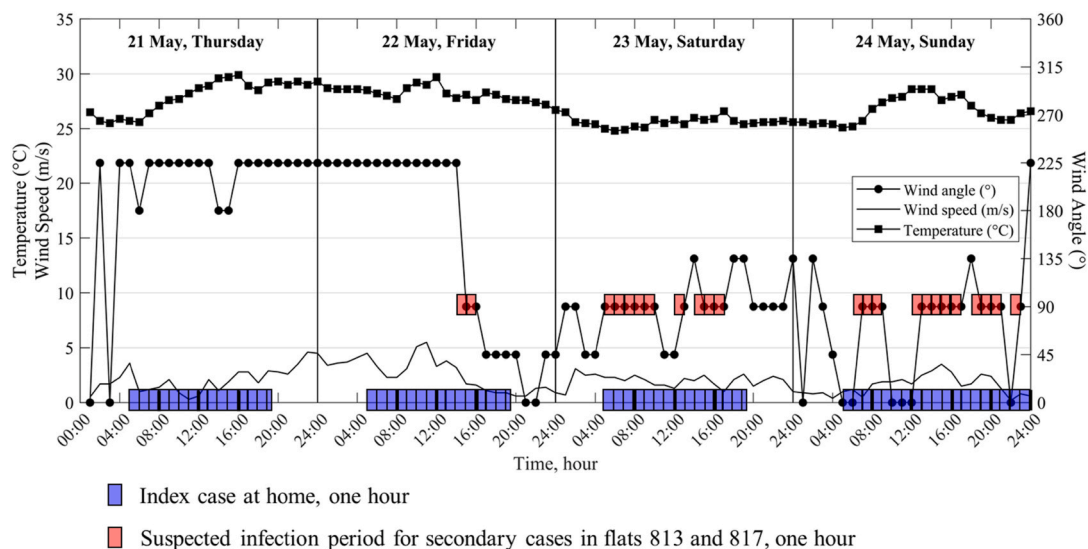
Fig. 2. Hourly temperature, wind speed and wind direction from 21 to May 24, 2020 at Shatin weather station (proximate to Luk Chuen House). Note that each light blue box on the x-axis indicates an hour for which the index case was at home, and one light red box on the wind direction plot indicates an hour in the suspected infection period for the secondary cases in flats 813 and 817 (that is, when the index case was at home and the hourly prevailing wind direction was easterly).
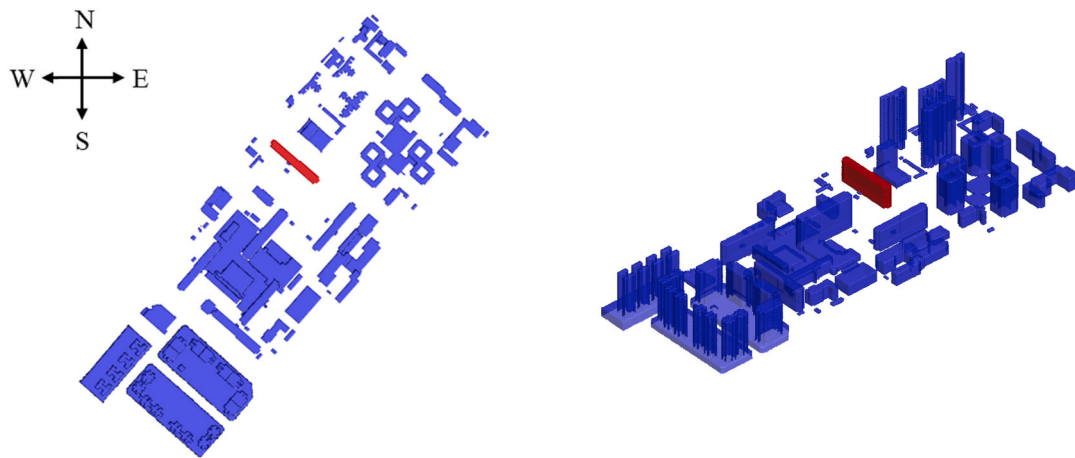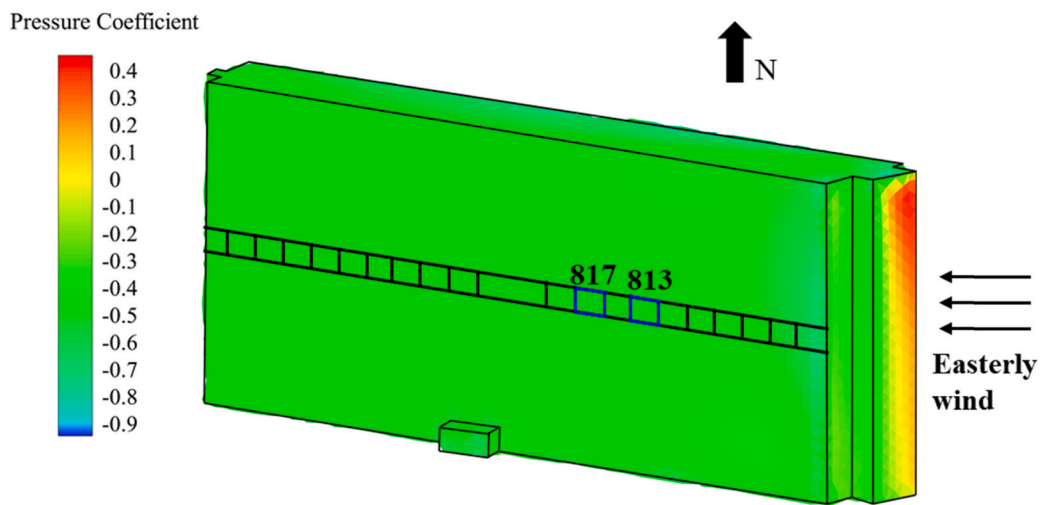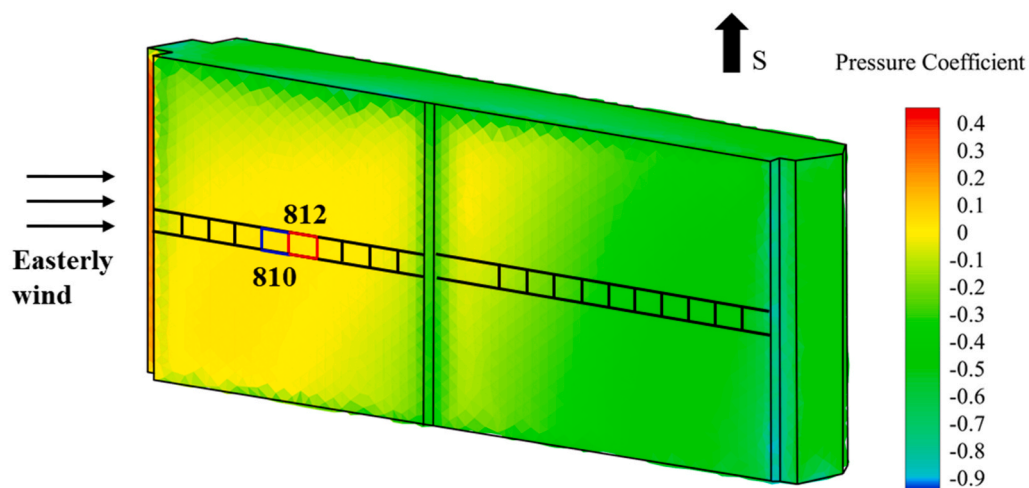
Fig. 3. Building layout in CFD simulation and the pressure contour on the surface of Luk Chuen House. (a) The layout of Luk Chuen House and 126 surrounding buildings in the CFD simulation (left: two-dimensional view from the top; right: a three-dimensional view), and the pressure contour on the surface of Luk Chuen House under an easterly wind from (b) the southern view and (c) the northern view.

22–24 May 2020 by a proximate weather station (Shatin Station) of the Hong Kong Observatory, a total of five major wind directions were simulated: northerly, north-easterly, easterly, south-easterly and south-westerly. Two pressure contours on the surface of Luk Chuen House under an easterly wind are shown in Fig. 3b and c. We conducted model validation and grid independence tests (Figs. S1, S2).

The wind coefficients were calculated as $(p - p_{ref})/(0.5\rho U_{ref}^2)$ [21], in which U_{ref} employs the incoming wind speed at a height of 10 m, (i.e., 1.70 m/s), and 10 m is the height of the anemometer in Shatin station. The predicted distributions of wind pressure coefficients on the external walls of the eighth floor of Luk Chuen House for different wind directions are displayed in Fig. 4. These wind pressure coefficients were subsequently used as input data for our multi-zone airflow simulation.

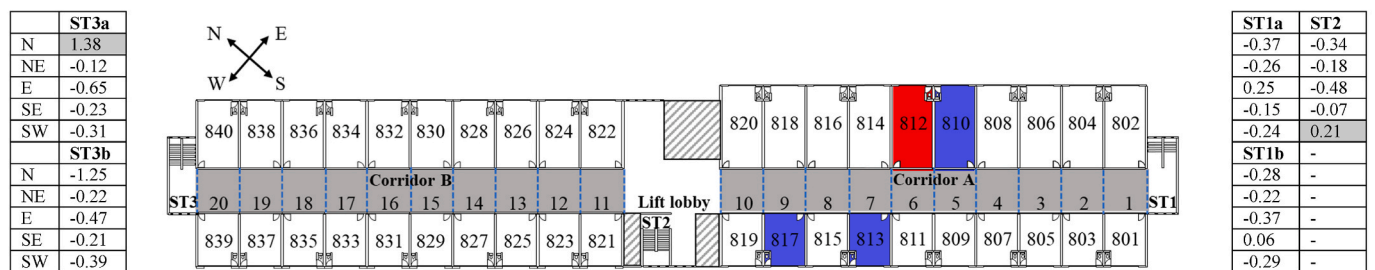The multi-zone airflow program (MIX) calculates airflow rates across the external wall of a building and between each zone inside the building based on mass conservation [22]. Specifically, MIX is based on the concept of mass balance and the modified Bernoulli's equation and can predict the airflow rate across the envelope and between the flats in a building. When it was used to predict the airflow between different flats in Block E of Amoy Gardens, where a major SARS outbreak occurred in 2003, MIX allowed for interpreting the associations between spatial infection patterns and the dispersion of SARS-CoV-containing aerosols [23]. More recently, MIX was used to calculate the concentrations of virus-laden aerosols and to estimate the infection risk via long-range airborne transmission in the first nosocomial outbreak of MERS-CoV in the Republic of Korea [24]. Note that Xiao et al. [24] estimated the infection risk employing the Wells-Riley equation. In this study, we concern only the relative magnitude of virus-laden aerosol concentration when we use the terms "infection risk" or "exposure risk", implicitly assume that all the bio-aerosol have equal viral load and all the residents have the same exposure time.

The detailed zone partitioning of the eighth floor of Luk Chuen House for MIX prediction is shown in Fig. S3. Besides the wind pressure coefficients, the air temperature and geometry of each zone at the time of exposure are also needed as input of the MIX program. A constant set of air temperatures was used for different zones, that is, 24.15 °C in the flat (27.15 °C in the kitchen and 27.25 °C in the toilet of flat 812), and 25.4–26.15 °C in the corridor, with a difference of 0.1–0.2 °C between neighbouring corridors (Table S1). Detailed definitions of the zones and their geometry are described in Supplementary Material S3.

The floors, ceilings, and walls inside the building were assumed to be perfectly sealed. We only considered leakage and openings to occur through windows and doors, which were modelled as porous openings uniformly distributed over a relatively large area [22]. The leakage coefficients were set at 0.4% for closed windows and 1.8% for closed doors [23,25]. Based on our on-site investigation, there was no exhaust fan in any of the accessible toilets as it was naturally ventilated; there was also no mechanical ventilation in each flat except for the air conditioning at the window between the kitchen and the main flat, which was assumed to be off during the simulation period. Aside from mechanical ventilation, particle deposition is also a mechanism by which airborne droplets are removed. The measured deposition loss rate coefficients [26] in a fully decorated room and an empty room were employed for flats and common areas (Table S4), respectively. Common areas include mean three stairwells, two corridors (Corridor A and Corridor B), and one lift lobby. Note that the airborne bio-aerosols have a diameter less than 10 μm and are emitted by coughing. The cough frequency, the number of droplets expelled per cough and size distribution of expelled droplets are the same as that in Ref. [24].

We noticed that several residents would leave the doors of their flats (that were connected to the corridor) ajar for cross ventilation. Thus, we evaluated the possible effects of door-opening on airflow in three

Flat	dir.	840	838	836	834	832	830	828	826	824	822	Lba	820	818	816	814	812	810	808	806	804	802
Window	N	1.24	0.98	0.75	0.55	0.35	0.22	0.12	0.03	-0.01	-0.03	0.05	-0.80	-0.33	-0.25	-0.21	-0.19	-0.19	-0.19	-0.19	-0.21	-0.25
	NE	-0.07	-0.05	-0.07	-0.10	-0.11	-0.11	-0.07	0.00	0.13	0.24	0.30	0.26	0.21	0.17	0.16	0.15	0.14	0.13	0.09	0.06	-0.06
	E	-0.58	-0.52	-0.49	-0.47	-0.44	-0.40	-0.36	-0.30	-0.24	-0.18	-0.10	-0.14	-0.05	-0.03	-0.00	0.01	0.02	0.02	0.02	0.00	-0.04
	SE	-0.31	-0.18	-0.14	-0.13	-0.11	-0.10	-0.09	-0.08	-0.06	-0.04	-0.03	-0.11	-0.07	-0.06	-0.06	-0.07	-0.08	-0.10	-0.13	-0.16	-0.24
	SW	-0.32	-0.32	-0.31	-0.29	-0.29	-0.29	-0.29	-0.29	-0.29	-0.29	-0.29	-0.29	-0.29	-0.29	-0.28	-0.28	-0.27	-0.27	-0.26	-0.26	-0.25
Fan	N	1.34	0.91	0.82	0.48	0.40	0.20	0.15	0.01	-0.00	-0.02	-	-0.99	-0.30	-0.26	-0.22	-0.20	-0.19	-0.19	-0.20	-0.20	-0.27
	NE	-0.10	-0.05	-0.06	-0.10	-0.11	-0.10	-0.09	0.05	0.09	0.27	-	0.27	0.20	0.17	0.16	0.15	0.15	0.14	0.09	0.06	-0.16
	E	-0.63	-0.51	-0.50	-0.47	-0.45	-0.40	-0.37	-0.29	-0.26	-0.16	-	-0.20	-0.05	-0.03	0.00	0.01	0.02	0.02	0.02	0.01	-0.09
	SE	-0.42	-0.17	-0.15	-0.12	-0.12	-0.10	-0.09	-0.07	-0.07	-0.04	-	-0.14	-0.06	-0.06	-0.07	-0.07	-0.09	-0.09	-0.14	-0.15	-0.22
	SW	-0.31	-0.32	-0.31	-0.29	-0.29	-0.29	-0.29	-0.29	-0.28	-0.29	-	-0.30	-0.29	-0.29	-0.28	-0.28	-0.27	-0.27	-0.26	-0.26	-0.24

	ST3a
N	1.38
NE	-0.12
E	-0.65
SE	-0.23
SW	-0.31
	ST3b
N	-1.25
NE	-0.22
E	-0.47
SE	-0.21
SW	-0.39

Floor plan: N/E/W/S compass. Upper row flats: 840 838 836 834 832 830 828 826 824 822 — 820 818 816 814 **812** **810** 808 806 804 802. Lift lobby. ST3, ST2, ST1. Corridor B, Corridor A. Lower row flats: 20 19 18 17 16 15 14 13 12 11 — 10 9 8 7 6 5 4 3 2 1; 839 837 835 833 831 829 827 825 823 821 — 819 **817** 815 **813** 811 809 807 805 803 801.

	ST1a	ST2
	-0.37	-0.34
	-0.26	-0.18
	0.25	-0.48
	-0.15	-0.07
	-0.24	0.21
	ST1b	
	-0.28	-
	-0.22	-
	-0.37	-
	0.06	-
	-0.29	-

Flat	dir.	839	837	835	833	831	829	827	825	823	821	Lbb	819	817	815	813	811	809	807	805	803	801
Window	N	-0.60	-0.61	-0.63	-0.64	-0.64	-0.62	-0.59	-0.53	-0.48	-0.42	-0.30	-0.23	-0.20	-0.17	-0.15	-0.14	-0.13	-0.13	-0.12	-0.12	-0.15
	NE	-0.20	-0.20	-0.20	-0.19	-0.19	-0.19	-0.19	-0.19	-0.19	-0.18	-0.18	-0.18	-0.18	-0.18	-0.18	-0.18	-0.19	-0.19	-0.19	-0.20	-0.20
	E	-0.47	-0.48	-0.48	-0.47	-0.47	-0.48	-0.48	-0.48	-0.48	-0.48	-0.47	-0.47	-0.47	-0.46	-0.46	-0.45	-0.45	-0.44	-0.46	-0.50	-0.63
	SE	-0.20	-0.14	-0.13	-0.12	-0.11	-0.10	-0.10	-0.09	-0.09	-0.08	-0.06	-0.04	-0.03	-0.03	-0.02	-0.02	-0.01	-0.01	0.00	0.00	0.00
	SW	0.16	0.27	0.31	0.31	0.30	0.30	0.28	0.28	0.26	0.25	0.17	0.12	0.09	0.06	0.03	-0.01	-0.04	-0.07	-0.10	0.14	-0.19
Fan	N	-0.60	-0.62	-0.63	-0.64	-0.64	-0.61	-0.60	-0.52	-0.49	-0.42	-	-0.25	-0.18	-0.18	-0.14	-0.14	-0.12	-0.13	-0.12	-0.12	-0.17
	NE	-0.20	-0.20	-0.20	-0.19	-0.19	-0.19	-0.19	-0.19	-0.19	-0.18	-	-0.18	-0.18	-0.18	-0.18	-0.18	-0.19	-0.19	-0.19	-0.20	-0.21
	E	-0.47	-0.48	-0.48	-0.47	-0.47	-0.48	-0.48	-0.48	-0.48	-0.48	-	-0.47	-0.47	-0.46	-0.45	-0.45	-0.45	-0.44	-0.46	-0.49	-0.68
	SE	-0.22	-0.13	-0.13	-0.12	-0.11	-0.10	-0.10	-0.09	-0.09	-0.08	-	-0.04	-0.04	-0.02	-0.02	-0.01	-0.02	0.00	0.00	0.00	0.02
	SW	0.06	0.30	0.29	0.31	0.32	0.29	0.31	0.27	0.27	0.25	-	0.15	0.08	0.07	0.01	0.01	-0.06	-0.07	-0.12	-0.13	-0.25

Fig. 4. Predicted distributions of wind pressure coefficients at the external openings of the eighth floor of Luk Chuen House for different wind directions from the CFD. The wind directions (dir.) N, NE, E, SE and SW represent the northerly, north-easterly, easterly, south-easterly and south-westerly wind directions, respectively. Positive values are shown in grey.

different scenarios (Table 1). In each scenario, the windows connected to the corridors were assumed to be closed. We denote Scenario 1 [All doors closed], Scenario 2 [813 and 817 ajar] and Scenario 3 [803 and 807 ajar].

The MIX-estimated inter-zonal flow rates were used to estimate the zonal concentrations of aerosols originating from the index case, based on the mass balance of the aerosols. The infectious bio-aerosol was released by the index case in her flat, which was composed of a bedroom, a kitchen and a toilet. We assumed that during the exposure period (from 00:00 on 22 May 2020 to 24:00 on 24 May 2020), the index case stayed in her flat during her home hours, i.e., between her shifts (05:00–19:30 on 22 and 23 May) and on her day off (05:00–24:00 on 24 May). We also assumed that infectious aerosol emission rate was constant when the index case was home, and zero when she was out of home. We suspected that during the period when the index case was at home, the secondary cases in flats 813 and 817 became infected when the hourly prevailing wind direction was easterly.

3. Results

3.1. Predicted hourly aerosol concentration profiles

Fig. 5 displays the hourly normalised bio-aerosol concentration in flat 812 under the three scenarios, as well as the hourly normalised bio-aerosol concentrations in the corridors and the flats opposite and adjacent to flat 812 in Scenario 1. Note that the concentration used for normalization is the average bio-aerosol concentration in flat 812 during the index case's home hours in Scenario 1, and that all the normalised bio-aerosol concentration profiles are presented as percentages. Fig. 6 illustrates the net airflow through the internal openings of the 68 zones (flats and corridors) that were investigated, according to five different wind directions.

It would not be appropriate to present the absolute aerosol concentration profiles as the strength of the source of the aerosols and its variations are unknown. Hence, we specify a constant source of aerosols (for the index case of flat 812) in our simulation. The aerosol concentration in flat 812 is affected by ventilation, which varies according to background wind speed and direction. For each scenario in flat 812 (Table 1), we normalise the estimated aerosol concentration using the average aerosol concentration for Scenario 1 in flat 812 during the period when the index case was at home (Table S5). Note that the reference for normalization is an average value, instead of a maximum value, which justify that he normalised concentration fluctuates around 100% in flat 812 (Fig. 5a). In order for cross-corridor transmission to occur, the infectious aerosols must first escape into the corridor. As shown in Fig. 5b, when the wind direction is easterly, the corridors adjacent to flat 812 (i.e., corridors 1–10) experiences the highest aerosol concentrations excluding flat 812 (normalised concentrations, 6–12%) because this area is immediately downwind from flat 812. It is interesting that corridor adjacent to flat 812 remain uncontaminated or experience far lower levels of contamination when the wind blows in other directions. This finding confirms our suspected infectious periods.

When the wind blows in other directions, such as in a south-easterly direction, the adjacent corridors 1–5 may also be contaminated, but at lower levels. This explains why flats 811, 813, 815, 817, and 819 experienced the second highest aerosol concentrations (approximately 0.4–1.2%), while flats 801, 803, 805, 807, and 809 had lower concentrations (i.e., less than 0.2% or substantially lower) (Fig. 5d). Flat 811 is

directly opposite to flat 812 and therefore reports the highest concentrations among all the flats that are opposite to flat 812.

The corridor areas distant from flat 812 are also contaminated when the wind is easterly. However, these areas record lower concentrations of aerosols (mostly less than 0.6%, Fig. 5c). Thus, the aerosol concentrations in the flats that are distantly located from flat 812 are very low (mostly less than 0.06%) (Fig. 5f and g).

The hourly aerosol concentration in each flat is a result of the pattern of airflow as well as the ventilation conditions. For example, between 14:00 and 16:00 on 22 May, the wind direction is easterly (Fig. 2). Accordingly, the aerosol concentration profiles for flats 811, 813, 815, 817 and 819 increase as the contaminated airflow from flat 812 is directed into these flats through the corridor (Fig. 6c). In the meantime, there is no inflow of contaminated air from the corridor for flats 801, 803, 805, 807 and 809; hence, the bio-aerosol concentration in each of these flats is almost zero. However, between 11:00 and 12:00 on 23 May, the wind direction is north-easterly (Fig. 2), and the inter-zonal airflow in corridor A is reversed and the aerosol concentration in zones 46–50 increases (Fig. 6b). Due to a lower inflow rate, the peak profile for flats 801, 803, 805, 807 and 809 during these hours is not as high as that for flat 811, 813, 815, 817 and 819 between 14:00 and 16:00 on 22 May.

In comparison with the flats on the opposite side of corridor A, the flats adjacent to flat 812 display considerably lower exposure levels (<0.2%) and shorter risk periods (Fig. 5e). Aerosols from the corridor enter flats 814, 816, 818 and 820 only when the wind shifts from an easterly direction to other directions. As for flat 810, an increase in aerosol concentration is observed for a brief period from 20:00 to 24:00 on 22 May and from 21:00 to 24:00 on 24 May; this indicates a substantially lower possibility of horizontal airborne transmission for residents of this flat than for the residents of flats 813 and 817. Among corridors 1–20, corridors 6–10 present the highest bio-aerosol concentrations, excluding flat 812. These are followed by corridors 1–5 and 11–20, with zones 11–20 recording bio-aerosol concentrations trend that are relatively similar to those in zones 6–10 (Fig. 5b and c).
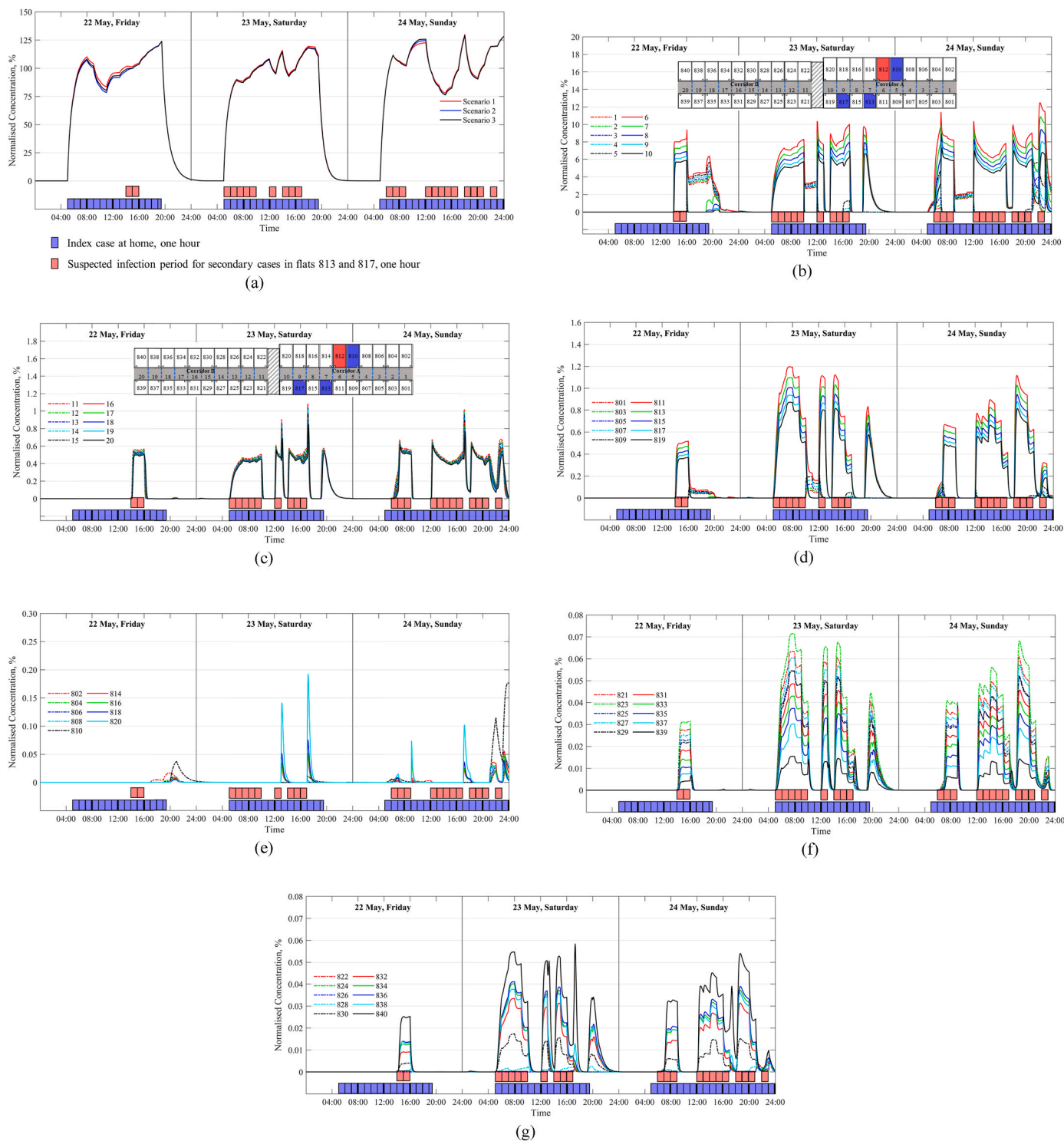
Comparison of the predicted inter-zonal airflow patterns from the MIX (Fig. 6) and the spatial infection pattern (Fig. 1) shows that the likely infection period for the secondary cases in flats 813 and 817 was the period when the wind direction was easterly and when the index case in flat 812 was at home (Fig. 6c). Furthermore, the hours in which the prevailing wind direction was northerly would have been deemed the safest period, in which the least number of residents in their flats (flat 802) were exposed to infection risk, and the region of exposure was almost confined to the corridor (Fig. 6a).

To verify MIX predictions, we compared the model data (Fig. 6e) with those in a related set of tracer gas experiment in Wang et al. [19]; see Fig. 7. There is a reasonable agreement.

It is observed that the corridor zones with high concentrations are on the windward side of the source room 812 under a southwesterly wind (Fig. 6e). The bio-aerosol concentration distribution at 24:00 on 24 May, was preceded with a time period when the wind direction is easterly (22:00–23:00 on 24 May). During 22:00–23:00 on 24 May, the bio-aerosols accumulate in the corridor 6–10. Subsequently at 23:00–24:00 on 24 May, the bio-aerosol concentrations in corridor 6-10 decrease. The airflow direction between flat 812 and corridor 6 during 23:00–24:00 on 24 May was bi-directional, which means virus-laden bio-aerosols still penetrated into corridor zones.

3.2. Spatial characteristics of exposure risk and the effects of door-opening

To elucidate the spatial characteristics of exposure risk, we group all the flats on the eighth floor (excluding flat 812) into eight areas in a clockwise direction and beginning from flat 801. Each area includes five flats or zones, except for area 7, which consists of four flats (flats 820, 818, 816 and 814) (Table S3 and Fig. S5). Accordingly, 20 zones in the two corridors are also grouped into four areas.

Table 1
Three simulation scenarios for the eighth floor of Luk Chuen House.

Scenario	Description
1	All doors of flats (that are connected to the corridor) are closed
2	Doors of flats 813 and 817 are ajar
3	Doors of flats 803 and 807 are ajar

Fig. 5. Normalised bio-aerosol concentration profiles. Plots show the normalised bio-aerosol concentration profiles (a) in flat 812 under the three different scenarios, (b) in adjacent corridor 1–10 (for flats 801–820) in Scenario 1 [All doors closed], (c) in remote corridors 11–20 (for flats 821–840) in scenario 1, (d) in the flats opposite to flat 812 in scenario 1, (e) in the flats adjacent to flat 812 in scenario 1, (f) in the flats distant from flat 812 and on the opposite side of the corridor in scenario 1, (g) in the flats distant from flat 812 and on the same side of the corridor in scenario 1. Note that the vertical axes of the seven plots differ in their ranges. Each light blue box and light red box indicates an hour for which the index case was at home and an hour during the period for potential secondary infections to occur, respectively (as Fig. 2). Note that for each scenario (Table 1), we "normalise" the estimated aerosol concentration using the average concentration for Scenario 1 in flat 812 during the period when the index case was at home, and some "normalised" values can be greater than 1.
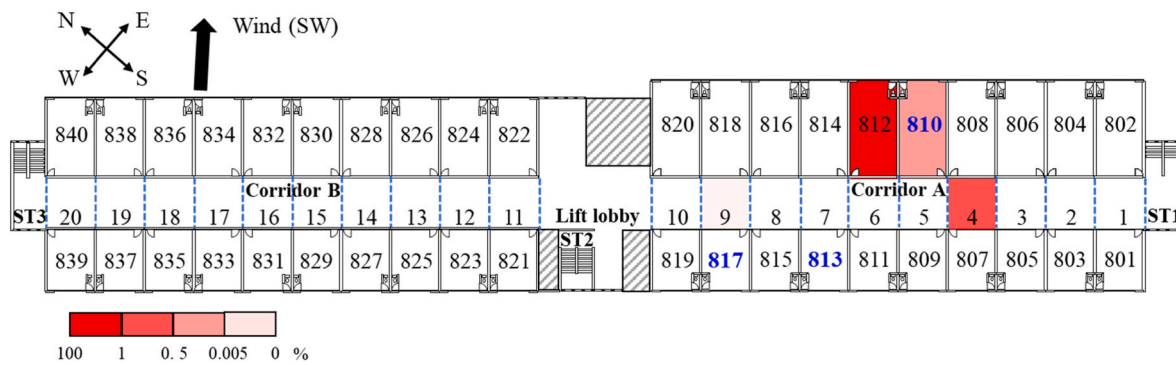
For the three scenarios, we calculate the average normalised bio-aerosol concentration in the 12 areas during the index case's home hours (Fig. 8a) and during the suspected infection hours for the secondary cases in flats 813 and 817 (Fig. 8b). In all three scenarios, the average concentration for the flats in area 2 is distinctly higher than that for flats in all other areas; this may explain why the residents of the flats in area 2 became infected while the others did not. Interestingly, the corridor zones show higher concentrations than the flats in area 2. We
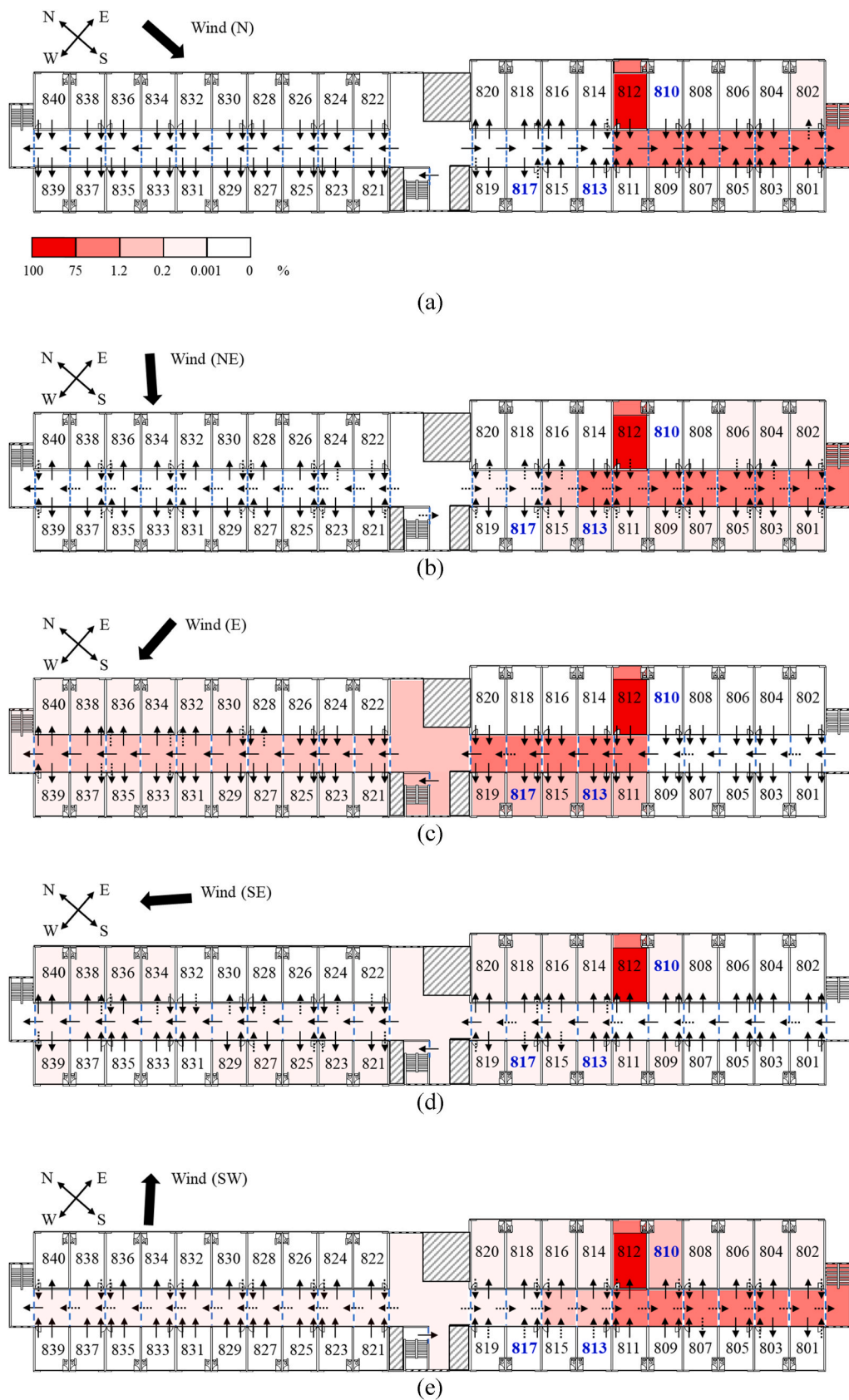
Fig. 6. Illustration of net airflow through the main internal openings and the normalised bio-aerosol concentrations (in %) at times characterised by different wind directions. Plots show the patterns of net airflow on the eighth floor of Luk Chuen House (under Scenario 1 [All doors closed].) with (a) a northerly wind at 11:00 on 24 May, (b) a north-easterly wind at 19:30 on 22 May, (c) an easterly wind at 15:00 on 22 May, (d) a south-easterly wind at 17:30 on 23 May, and (e) a south-westerly wind at 24:00 on 24 May in the year of 2020. The degree of transparency of the red square in each zone is inversely (but not proportionally) related to its normalised bio-aerosol concentration [refer to the colour scale in (a)]. The direction of net airflow is indicated by the black arrows, with a solid arrow indicating unidirectional airflow and a dashed arrow indicating bidirectional airflow.

Fig. 7. Normalised tracer gas concentrations (%) in flats 810 and 812 and the corridors near the meshed window of flats 808 and 817 monitored at 17:47 on June 17, 2020.
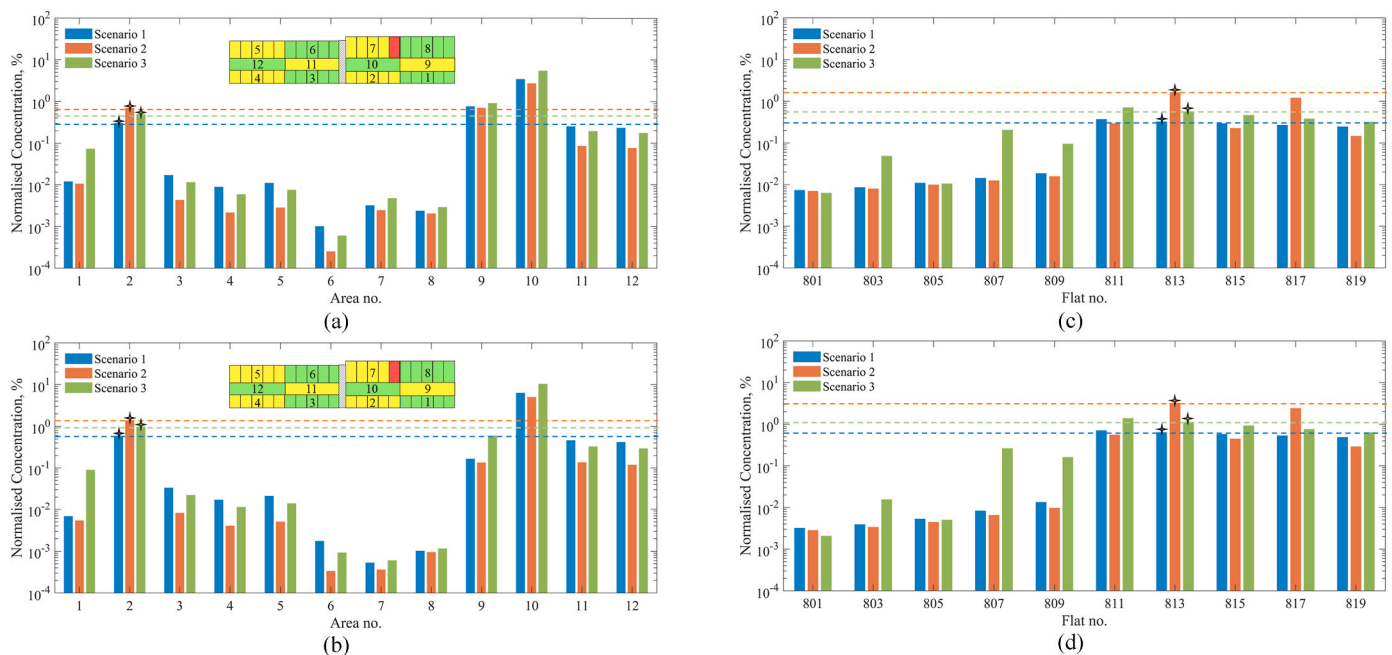
Fig. 8. Comparison of the average normalised bio-aerosol concentrations between the 12 areas, and between the flats in area 1 and area 2, under the three scenarios. (Scenario 1 [All doors closed], Scenario 2 [813 and 817 ajar] and Scenario 3 [803 and 807 ajar]). Plots show the average normalised bio-aerosol concentrations for (a) the 12 areas during index case's home hours, (b) the 12 areas during suspected infection period for the secondary cases in flats 813 and 817, (c) the flats in area 1 and area 2 during the index case's home hours, and (d) the flats in area 1 and area 2 during the suspected infection period for the secondary cases in flats 813 and 817. Note that values on the y-axis are presented on a log scale and the blue, brown, and green dashed lines notifies the corresponding normalised concentration in flats of area 2 ([a] and [b]) or flat 813 ([c] and [d]) in Scenario 1, 2, 3, respectively.

expect that the residents spent most of their time in their own flats. All other flat areas did not register any infections.

We also obtain the average bio-aerosol concentrations for flats directly opposite to flat 812 under the three scenarios (Fig. 8c and d). This allows for examining the impact of door-opening on a resident's exposure to aerosols. In contrast to Scenarios 1 and 3, in which the bio-aerosol concentrations of flats in area 2 decrease from flat 811 to 819, under Scenario 2, the average bio-aerosol concentrations in flats 813 and 817 exceed those in flats 811, 815 and 819 (Fig. 8c and d), due to an increased effective leakage area and higher ventilation rate. The air change rates in flats 813 and 817 increase by 0.9–13 (mean: 3.53) in scenario 2 [813 and 817 ajar] compared to scenario 1 [All doors closed], which brings in more virus-laden aerosols (Fig. 9). We speculate that the residents of flats 813 and 817 may have opened the doors or windows that connected their flats to the corridor and were thus exposed to higher exposure risks than the residents of flats 811, 815 and 819. Nonetheless, this remains a speculation because we have no information on door-opening behaviour and the exact virus release period in this study. In

Scenario 3, when the residents of flats 803 and 807 open the doors connecting their flats to the corridor for 20% (effective leakage area, ELA), the air change rates in flats 803 and 807 increase by 0.9–7.6 (mean: 3.12) h^{-1} compared to scenario 1 [All doors closed] and the aerosol concentrations in flats 803, 807 and 809 increase but remain substantially lower than those in flats in area 2, which also increase due to door-opening of flats 803 and 807.

4. Discussion

4.1. Horizontal transmission is likely caused by cross-corridor airflow and insufficient ventilation

The secondary infections in flats 813 and 817 were probably caused by the cross-corridor airflow from flat 812, where the index case lived. Using the hourly wind data, we inferred the most likely periods of exposure for residents in Luk Chuen House. The local health authorities could not identify any possible encounters between the secondary
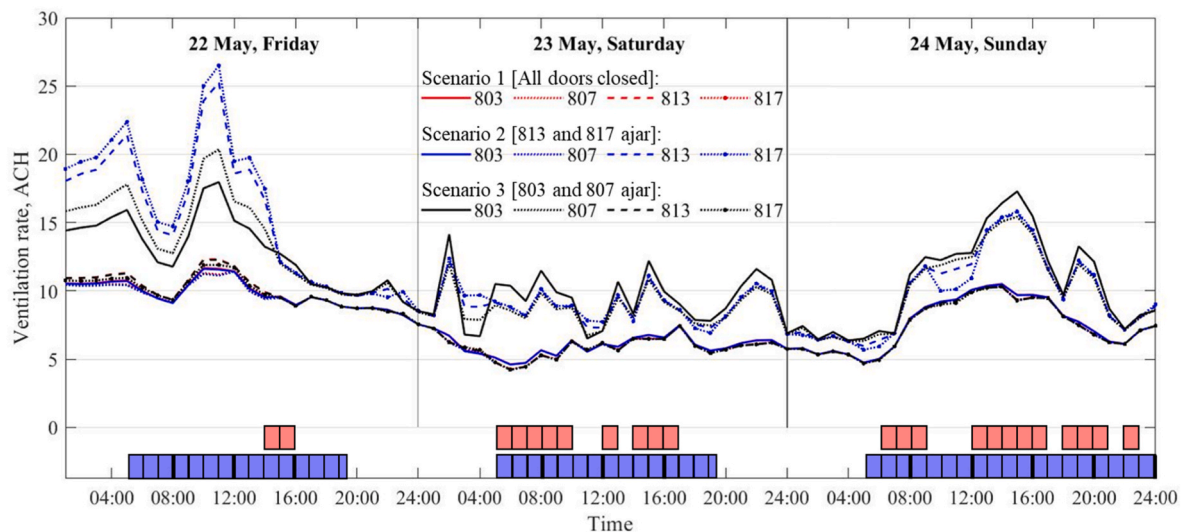
Fig. 9. Estimated hourly ventilation rates (ACH) for flats 803, 807, 813, and 817 in 3 scenarios, derived from the MIX program.

infected individuals and the index case. Although residents may have shared the same lifts or walked past each other in the corridor, the index case's work activity patterns (i.e., working the nightshift) would have reduced likelihood of such events happening. Except for the resident of flat 810, no other residents of flats that were on the same side of the corridor as flat 812 experienced secondary infections. This pattern of spatial infection agrees with our modelled pattern of airflow (Fig. 6).

It may be useful to reiterate the roles of two connected drainage stacks in facilitating the vertical spread of the virus [19]. There are 20 pairs of connected drainage stacks in the building: for example, the pair of stacks for −10 and −12 flats discharge wastewater from all −10 and −12 flats. The viral aerosols in the vertical stack may have originated from the washbasin or toilet of flat 812, before it was transported by the stack pair, and leaked into flats 810, 710 and 1112. No other flats that were connected by other stack-pairs were contaminated, except for flats 813 and 817, which form a horizontal spatial cluster with flat 812.

The results of our simulation suggest that flats in area 2 that were located downstream of flat 812 when the wind direction was easterly during 22–24 May had the highest exposure risk, while all other flats had a low exposure risk (Fig. 8a and b). This aligns with the observed spatial pattern of infections. Two flats in area 2 had secondary infections, while all flats in the other areas did not (except for flat 810, which belonged to the vertical cluster was the result of contamination via the shared connected drainage stacks; [19]. We cannot rule out the possibility that the two infected neighbours once physically encountered the index case or touched common surfaces that were contaminated. The two residents who contracted COVID-19 in flats 813 and 817 were 68 and 78 years old, respectively. They might have spent more time at home; this would result in a longer exposure duration and a higher probability of overlapping with periods during which the index case was in her flat.

Our results showed that door-opening may have also played a role in the cross-corridor transmission of SARS-CoV-2. If they opened their corridor doors by 20% (effective leakage area, ELA), the residents of flats 813 and 817 would have had an exposure risk that was greater than four times that of the residents of other flats in area 2 (Fig. 8c and d).

The index case was the only virus-laden aerosol source in this outbreak, and it was assumed that she remained in her bedroom throughout the entire period for which she was home. Our results suggest that when the wind direction was south-easterly (e.g., 18:00–19:00 on 23 May) or south-westerly (23:00–24:00 on 24 May), the airflow through the door and window of flat 812 would have been a unidirectional inflow. This would have been the desirable situation for the flats opposite to flat 812; the aerosol concentration in these flats would also

have diminished rapidly during the hours for which the prevailing wind direction was south-easterly or south-westerly (Fig. 5d). Nevertheless, this would have been an undesirable situation for the flats adjacent to flat 812 because the residual aerosols in the corridor would have been transmitted into these flats during these hours (Fig. 5e).

The coexistence of vertical and horizontal clusters as observed in Luk Chuen House is not new. Both a vertical and horizontal spread was documented during the 2003 Amoy Garden SARS-CoV outbreak [27], which included a transmission across the corridors on each floor in Block E of the estate [23].

Besides the studies reviewed in the Introduction, several studies have reported outbreaks of respiratory infections that were transmitted between rooms. For instance Ref. [28], described a tuberculosis (TB) outbreak in a hospital. They found that the droplet nuclei of a draining abscess from a TB patient in a positive pressure room dispersed into the corridor and subsequently to other rooms. The corridor ventilation rate was low, and there was a likelihood that the intake of air from outdoors decreased or ceased due to the cold outdoor weather at the time. Similarly, Gustafson et al. [29] described a chickenpox outbreak among children in a hospital, with all exposure occurring within one afternoon. The index case remained in strict isolation but was unfortunately placed in a positive pressure room.

These studies have demonstrated the combined roles that ventilation rates and room air pressure play in shaping the outbreaks of respiratory infections. Specifically, low ventilation in the index patient's room led to an accumulation of highly infectious air, while positive pressure – due to either the setup of a room or wind conditions at the time – leaked the infectious air into a poorly ventilated corridor. At the time of revision (early March 2022), the Omicron variants have been rapidly spreading in Hong Kong, particularly in public housing with both horizontal and vertical transmission are suspected to play a role [30].

4.2. The dual roles of airflow

Strictly speaking, still air does not transport aerosols. As airflow transports aerosols that are suspended in the air, it is airflow that transmits or carries airborne particles from one location to another. This is referred to as the 'transport role' of the airflow. In addition, the inflow of clean air into a space will dilute any polluted air, and the outflow of polluted air will remove aerosols from the space. This is referred to as the 'removal role' of the airflow. For any given airflow, the removal role is associated with the transport role. If polluted air is removed not by transportation of the air to the external environment, but to a neighbouring indoor space, then the effect of removal on a space will bring an

effect of pollution on another space. This phenomenon involving the expelling of pollutants from one room and the transporting of the same pollutants to other rooms, for which we refer to as the 'dual roles of airflow'.

Understanding the dual roles of airflow is crucial to infection control. In a corridor-based hotel setting, the settings shown in Fig. 10a (left) and 10b (left) will be ideal for quarantine hotels in which such naturally driven flows exist. Fig. 10a and b (middle and right) show possible pollution situations depending on natural wind directions that drive cross-corridor ventilation; this occurs in Luk Chuen House. Obviously, such flows of infiltration or natural ventilation exist when the building envelope is not airtight. For simplicity, the bi-directional flows across doorways or windows (which exist when there is a sufficient buoyancy effect) are not shown in Fig. 10. Note that the difference between the middle and right plots of Fig. 10a and b is the ventilation rate that is represented by the arrow width.

The dual roles of airflow discussed above may provide at least two suggested approaches for controlling the spread of infections in hotel-like settings. These approaches correspond to two different scenarios – when the building envelope is airtight, and when it is not.

When the building envelope is not airtight, sufficient dilution can be used for infection control. In the case of air pollution, the levels of airborne pollutants can be diluted to sufficiently low levels with sufficient ventilation (Fig. 10b right). In theory, there is no need to worry about the transport of the aerosols by airflows if sufficient ventilation is available. The challenge lies in determining the exact ventilation rate that suffices for infection control; this question remains to be answered.

When the building envelope is airtight, we can use the isolation principle to minimise the negative effect of the transport role, that is, by isolating the contaminated air. This can be achieved by creating a positive pressure in the corridor and making it well ventilated (Fig. 10c). In addition to introducing outdoor air to establish positive pressure, the corridor air may be cleaned by filtration and Ultraviolet germicidal irradiation (UVGI) devices. The removal of infectious aerosols differs from the removal of gaseous air pollutants, as aerosols can also be removed by filtration and disinfection such as UVGI. Therefore, each individual guest room may also be equipped with filtration and UVGI.

4.3. Ventilation in quarantine hotels

The infection scenario discussed in the present study should be similar to instances of guest-to-worker or between-guest infections
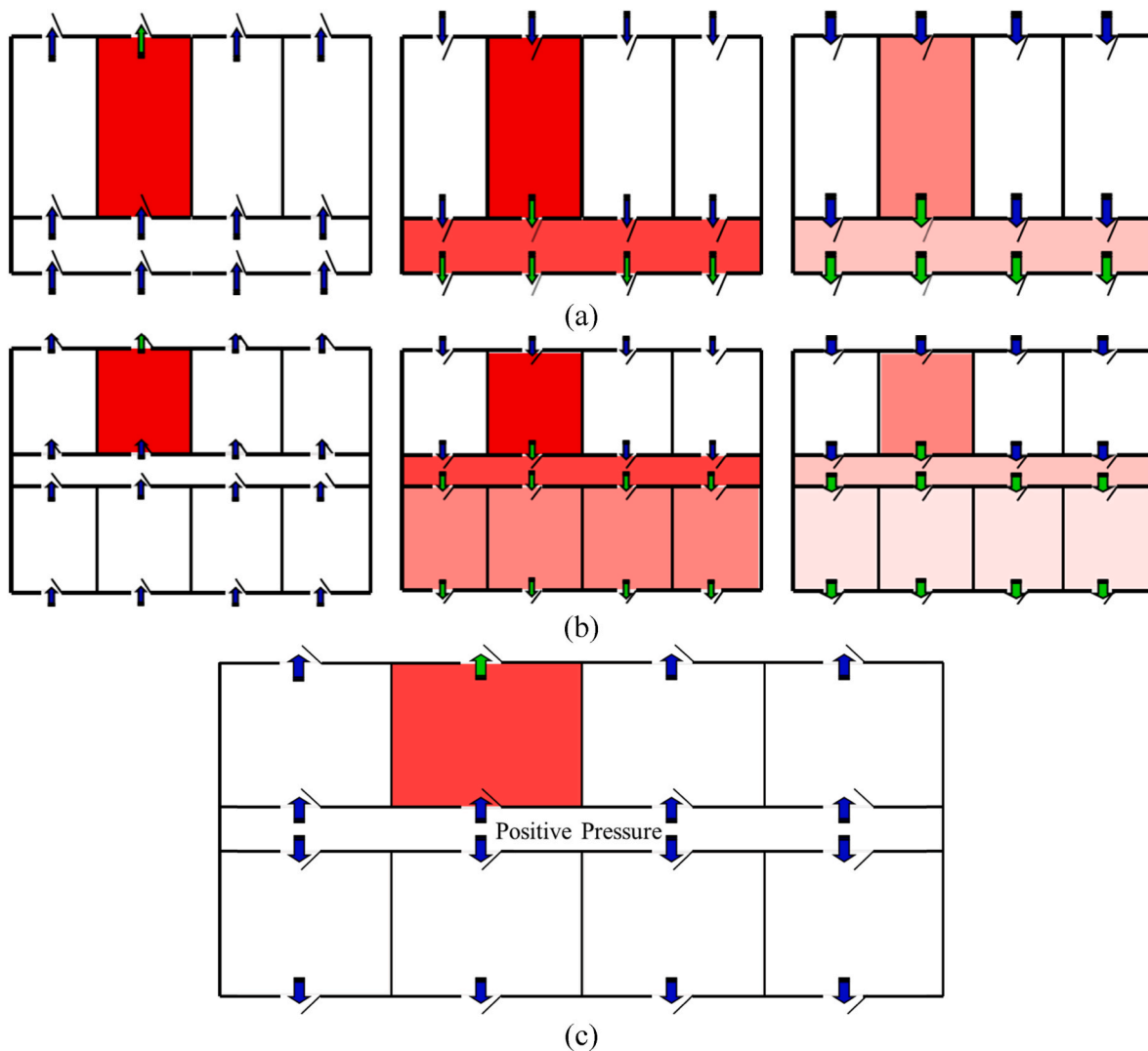
Fig. 10. Schematic diagram of airflow in typical hotel floorplans under different ventilation scenarios. Each small square represents a guest room. The guest room with the index case is always the second room in the top row of each plot. A corridor or guest room that is subsequently polluted is shown in lighter red. The uncontaminated space is shown in white. Green arrows represent the rate and direction of airflow, with arrow widths corresponding to airflow rates. The individual plots show airflow for (a) a floorplan featuring a side corridor, (b) a floorplan featuring a central corridor, and (c) a floorplan where sufficient positive pressure in the corridor prevents the escape of polluted air from the room of the index case into the corridor.

documented in quarantine hotels that have floorplans similar to that of Luk Chuen House. The inter-zonal flows driven by winds, buoyancy and mechanical ventilation into each room (e.g., the bathroom fans in a hotel room) have the potential to spread viral particles. More infections can occur when the corridor is poorly ventilated (e.g., Fig. 10a and b, middle) than when it is sufficiently ventilated (Fig. 10a and b, right). If both the guest rooms and the corridor are well ventilated, the infection risk is low. If the corridor has a sufficiently strong positive pressure, then in theory no infection should occur (i.e., assuming airborne transmission is the predominant transmission route) (Fig. 10c). The fact that some items such as quilts, pillows and towels can be contaminated suggests that hotel service personnel may be exposed to infection risk due to the resuspension of particles, followed by inhalation.

McKendrick and Emond [31] presented an intriguing study of the cross-infection risks of chickenpox and measles in seven hospitals with different floorplans. These authors recommended floorplans featuring lateral corridors and cautioned against those featuring central corridors. They also proposed that air from a patient's room should not be discharged into any corridors and found that the movement of patients and door-opening increased cross-infection risk. Anderson et al. [32] showed that floorplans featuring patient rooms with negative pressure (i.e., corridors with positive pressure) helped to reduce infections in hospitals. Another study showed that higher ventilation rates led to fewer common cold infections in crowded student dormitories in China [33]. Many student dormitories in China as well as those in other countries also feature long central corridors like those found in hotels. These studies in hotels and student dormitories have revealed the design characteristics and human behaviours that can help to minimise cross infections: lateral corridors, airflow from corridors to guest rooms, sufficient ventilation, the prohibition or reduction of human movements outside of the guest room, and the minimisation of periods in which the doors of opposite or adjacent rooms are open.

Two users of a quarantine hotel in the UK [34] reported that while they could participate in outdoor exercises, there was a possibility of meeting other quarantined occupants in the corridors. The occupants also opened their doors within seconds of each other to receive delivered food. This was not the experience of one of the present study's authors (Li), who stayed in quarantine hotels in mainland China and Hong Kong. There were, however, occasions on which test samples were taken, and the doors of the opposite rooms were open within the same period (as the medical team had multiple staff taking samples from different rooms simultaneously). On these occasions, the occupants had to remove their masks for oral or nasal sampling.

There are several methods for minimising the leak of air from a room into a corridor. The necessary condition for preventing a leak is that the air pressure of the corridor is always higher than that of the room, that is, a positive pressure is maintained at the corridor. This can be achieved by providing a sufficient supply of air to the corridor. The volume of additional air required may be estimated based on the worst possible pressure profile, which is determined by the air temperatures in the guest rooms and the corridor (e.g., Fig. 11) as well as the wind direction. In summer, a cooler temperature may be set in the guest room for human comfort (Fig. 11c and d). In such a situation, the worst pressure profile is created when positive wind acts on the window (Fig. 11c). The wind pushes the neutral plane in the opposite direction, allowing more air to escape into the corridor. A greater effort is needed to push the neutral plane down to the floor level. Under a windier condition, a cooler temperature in the corridor may be the more suitable choice. The worst condition is also shown in Fig. 11a when the room temperature is higher than that in the corridor. The required over-supply of airflow to the corridor is also a function of the volume of air that is leaked from the door and the window. A multi-zone airflow program such as MIX (which was used in the present study) can be used for designing room or corridor temperature and opening geometry.

4.4. Challenges in improving ventilation in public housing in Hong Kong

Although the focus of discussion in this paper centres on quarantine
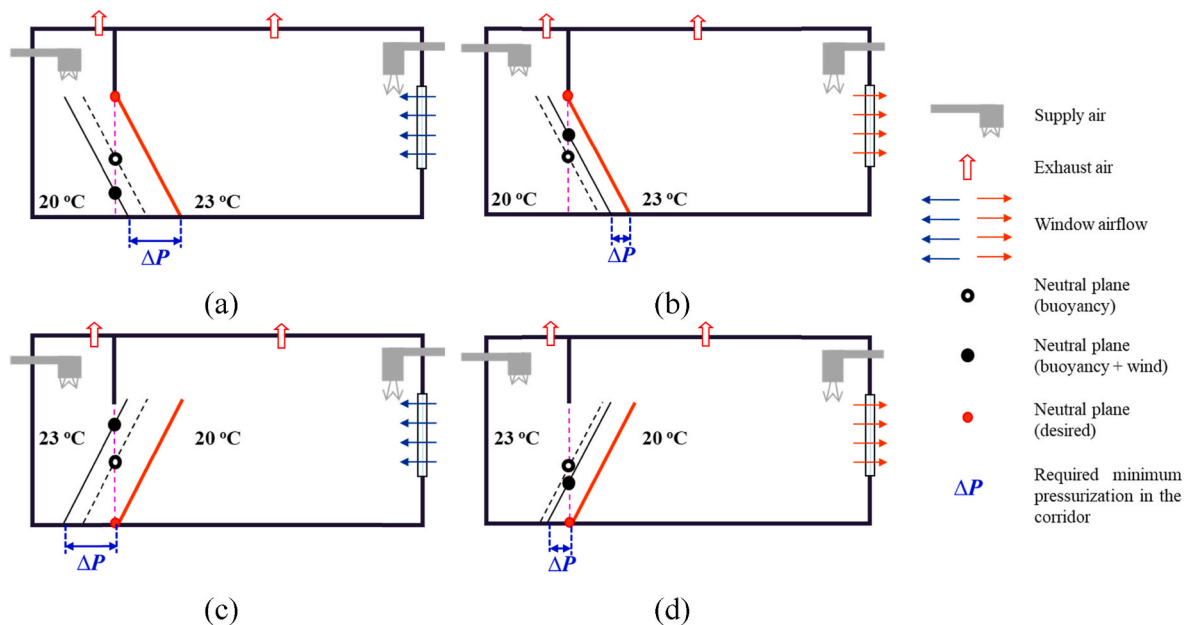

Fig. 11. Estimating the need for an imbalance in airflow or the over-supply of air to the corridor to avoid the escape of air from a guest room to the corridor. The ΔP as shown in all plots is the minimum required pressurization in the corridor. The goal of design is to push the neutral plane at the doorway up or down such that no air is leaked from the room to the corridor (desired pressure profile: indicated by the solid red line). The neutral plane is located at mid-height when only a buoyancy force from differences in air density exists (buoyancy-driven pressure profile: indicated by the dotted line). When wind pressure also acts on the window, the neutral plane moves (wind- and buoyancy-driven pressure profile: indicated by the solid black line). Individual plots illustrate the movement of the neutral plane when (a) the guest room is warmer than the corridor, and a positive wind acts on the window, (b) the guest room is warmer than the corridor, and a negative wind acts on the window, (c) the guest room is cooler than the corridor, and a positive wind acts on the window, and (d) the guest room is cooler than the corridor, and a negative wind acts on the window.

hotels, the studied COVID-19 outbreak occurred in a public housing building in Hong Kong. Thus, our findings also provide insights for improving ventilation in public housing in Hong Kong. Furthermore, many older buildings intended for public housing in Hong Kong were not originally designed to accommodate air conditioning (as this technology was not available at the time). In 2020, 45% of the population in Hong Kong live in public permanent housing [35]. According to Lu et al. [36]; 69.4% of COVID-19 patients in Hong Kong were residents of public housing.

The layout of Luk Chuen House is the same as that of Wing Shui House, which was studied by Niu and Tung [37]. Their study measured the ventilation rate of the building and revealed the roles of both transport and removal of the corridor air at both ends of the corridor, which were well ventilated, as well as at the middle of the corridor, where the lift lobby was located. A similar effect of ventilation in a cross-corridor floorplan ventilation was documented by Mu et al. [38, 39]. The positive effect of the balcony on the ventilation and contaminants dispersion in a naturally ventilated building was studied by Cui et al. [40]. It was unfortunate that the flat of the index case at Luk Chuen House and the two flats of the secondary infected cases were located at the middle of the exact section of the corridor where ventilation was at its worst when the wind blew in an easterly direction. Ventilation rates in an almost identical floor plan on the thirteenth floor in a 16-storey public housing building were measured by Wu et al. [41,42]. Interestingly, the same authors [41] previously predicted that flats downstream from a source of contaminants would experience a significant infection risk. Our findings for the horizontal spatial cluster in the COVID-19 outbreak at Luk Chuen House confirm these predictions.

There is an urgent need to improve ventilation in public housing. At Luk Chuen House, we observed that many residents had placed objects that obstructed the airflow from the meshed windows of their flats to the corridor. Such old public housing buildings were designed and constructed during the period when air conditioners were not yet widely used. Air conditioners had since been installed in almost all flats, and to save energy when their air conditioning was switched on, the residents would often shut the windows and any openings of their flats. However, we found that the openings in the walls at the two ends of the corridor and at the central lift lobby area provided insufficient ventilation for the corridor. When airflow was obstructed at the doors and meshed windows of the flats upwind, the ventilation in the corridor would become poor, and the flats downwind would not be well ventilated. It would be very difficult to ensure adequate ventilation in such situations. A well-ventilated corridor is essential for minimising the cross-corridor transmission of infectious viruses and other airborne pollutants. One possible solution is to seal the corridor (i.e., by sealing the openings at the two ends of the corridor and the centre lift lobby with an operable airtight window), and to install a positive pressure ventilation system for the corridor.

4.5. Limitations

We recognise several major limitations of the study. First, the field experiment was conducted in a very short period; the research team was only provided with access to the premises for two days [19]. The team had no access to the flats opposite to flat 812 on the eighth floor. It was not possible to take direct measurements of the tracer gas concentrations in flats 813 and 817, although we placed a sensor near the meshed window of flat 813, which was accessible from the corridor. In addition, the prevailing wind directions during the field experiment differed from the easterly wind direction that prevailed during the suspected period of exposure. Thus, the estimates of exposure risk were based on a multi-zone airflow model.

Second, our study lacked information on the behaviour of the residents, including the exact times at which they stayed in their flats during the suspected exposure period, whether and how often they opened the doors and windows of their flats, and their use of air-conditioning. The latter two factors would have influenced the air temperatures in their flats, which may have affected the buoyancy effect and inter-zonal flows. Given that the affected flats on the eighth floor of the building are in relatively open surroundings, their airflow is likely predominantly driven by wind, and the buoyancy effect is not expected to be significant.

Third, the CFD-predicted pressure coefficients are for a sealed building, which may lead to errors in the predicted airflow rates by MIX [43]. However, an early study showed that when the wall porosity is less than 10–20% of the wall area (Seifert et al., 2006), such as sealed building approach can provide reasonably accurate results.

5. Conclusion

In the COVID-19 outbreak at Luk Chuen House, cross-corridor airflows may explain the spread of SARS-CoV-2-laden aerosols from the flat where the index case lived to two flats on the other side of the central corridor. During the suspected period of exposure – that is, the day of and two days following the symptoms onset in the index case – a prevailing easterly wind resulted in a high concentration of viral aerosols in flats 811, 813, 815, 817 and 819. Flats 814, 816, 818 and 820, which were on the same side of the corridor, had aerosol concentrations that were approximately 2 orders of magnitude lower than that in the flat of the index case. Other flats on the same floor that were distantly located from the flat of the index case (e.g., 822, 824, 826, and 828) were almost risk-free. When the doors of flats 813 and 817 that connected to the corridor were open, the residents of these flats experienced the highest exposure risk, which was higher than that experienced by the residents of flats 811, 815 and 819. The results from our computer modelling align with the observed patterns of spatial infection in the horizontal cluster of the outbreak. It will be a challenge to improve ventilation conditions in similar public housing buildings. However, portable air cleaners with high efficiency particulate air (HEPA) filtration or ultraviolet germicidal irradiation (UVGI) may be applied.

Following a detailed consideration of the dual roles of airflows in long-corridor buildings – that is, the removal and transport roles – we identify two distinct strategies for controlling the spread of airborne infections in such buildings. The first is to provide sufficient ventilation in all areas, such that the transport of infectious aerosols is no longer an issue. This may be feasible with well-designed and naturally ventilated buildings. The second strategy is to control the transport of infectious aerosols, such as by controlling the direction of airflow between rooms.

The cross-corridor transmission investigated in the present study appears to reflect the outbreak patterns of COVID-19 infections in quarantine hotels worldwide. Most of these quarantine hotels were not originally designed for quarantine purposes. We therefore recommend that, if available, single-sided corridor hotels with the right prevailing wind directions are more suited to the purposes of quarantining cases of airborne infections. In hotels with central corridors, the maintenance of positive pressure and sufficient ventilation in the corridor must be ensured to help reduce infections.

CRediT authorship contribution statement

Pan Cheng: Data curation, Formal analysis, Investigation, Methodology, Visualization, Writing – original draft. **Wenzhao Chen:** Methodology, Writing – review & editing. **Shenglan Xiao:** Methodology, Writing – review & editing. **Fan Xue:** Methodology, Writing – review & editing. **Qun Wang:** Methodology, Writing – review & editing. **Pak Wai Chan:** Methodology, Writing – review & editing. **Zhang Lin:** Data curation, Writing – review & editing. **Jianlei Niu:** Data curation, Writing – review & editing. **Yuguo Li:** Conceptualization, Funding acquisition, Methodology, Writing – original draft, Writing – review & editing.

Declaration of competing interest

The authors declare that they have no known competing financial interests or personal relationships that could have appeared to influence the work reported in this paper.

Acknowledgements

Appendix A. Supplementary data

Supplementary data to this article can be found online at https://doi.org/10.1016/j.buildenv.2022.109137.

References

[1] Y. Li, H. Qian, J. Hang, X. Chen, P. Cheng, H. Ling, M. Kang, Probable airborne transmission of SARS-CoV-2 in a poorly ventilated restaurant, Build. Environ. 196 (2021), 107788.

[2] X. Li, H. Chen, L. Lu, L.L. Chen, B.P.C. Chan, S.C. Wong, V.C.C. Cheng, K.Y. Yuen, K.H. Chan, K.K.W. To, High compliance to infection control measures prevented guest-to-staff transmission in COVID-19 quarantine hotels, J. Infect. S0163–4453 (21) (2021), 00533-00538.

[3] S.L. Miller, W.W. Nazaroff, J.L. Jimenez, A. Boerstra, G. Buonanno, S.J. Dancer, C. Noakes, Transmission of SARS-CoV-2 by inhalation of respiratory aerosol in the Skagit Valley Chorale superspreading event, Indoor Air 31 (2) (2021) 314–323.

[4] C. Ou, S. Hu, K. Luo, H. Yang, J. Hang, P. Cheng, Y. Li, Insufficient ventilation led to a probable long-range airborne transmission of SARS-CoV-2 on two buses, Build. Environ. 207 (2022), 108414.

[5] World Health Organization (WHO), Coronavirus disease (COVID-19): how is it transmitted?, 2021. Updated 23 December 2021, https://www.who.int/news-room/questions-and-answers/item/coronavirus-disease-covid-19-how-is-it-transmitted. (Accessed 10 March 2022).

[6] L.E. Leong, J. Soubrier, M. Turra, E. Denehy, L. Walters, K. Kassahn, C.K. Lim, Whole-genome sequencing of SARS-CoV-2 from quarantine hotel outbreak, Emerg. Infect. Dis. 27 (8) (2021) 2219–2221.

[7] CityNews, 2 quarantine hotels in the GTA hit with COVID-19 outbreaks. https://toronto.citynews.ca/2021/05/11/quarantine-hotel-covid-19-outbreak/, 2021. (Accessed 31 October 2021).

[8] G. Fernando, S. McPhee, Coronavirus: Victoria's new lockdown could cost $1 billion a week, Treasurer says. https://www.news.com.au/finance/economy/australian-economy/coronavirus-victorias-new-lockdown-could-cost-1-billion-a-week-treasurer-says/news-story/9d26f9986565aee82cfeb9623c0b0ee6, 2020. (Accessed 31 October 2021).

[9] British Broadcasting Corporation (BBC), Covid: 'Urgent' call to shut Reading quarantine hotel after outbreak. https://www.bbc.com/news/uk-england-berkshire-57417585, 2021. (Accessed 20 December 2021).

[10] S.C. Wong, H. Chen, D.C. Lung, P.L. Ho, K.Y. Yuen, V.C.C. Cheng, To prevent SARS-CoV-2 transmission in designated quarantine hotel for travellers: is the ventilation system a concern? Indoor Air 31 (5) (2021) 1295–1297.

[11] L. Grout, A. Katar, D. Ait Ouakrim, J.A. Summers, A. Kvalsvig, M.G. Baker, T. Blakely, N. Wilson, Failures of quarantine systems for preventing COVID-19 outbreaks in Australia and New Zealand, Med. J. Aust. 215 (7) (2021) 320–324.

[12] Public Health Expert (PHE), Australia's quarantine systems failures: lessons for NZ. https://sciblogs.co.nz/public-health-expert/2021/05/12/australias-quarantine-systems-failures-lessons-for-nz/, 2021. (Accessed 7 January 2022).

[13] Radio Television Hong Kong (RTHK), Experts suspect cross-infection at quarantine hotel. https://news.rthk.hk/rthk/en/component/k2/1606261-20210817.htm, 2021. (Accessed 31 October 2021).

[14] F.C. Jiang, L. Jiang, Z.G. Wang, Z.H. Meng, S.F. Shao, B.D. Anderson, M.J. Ma, Detection of severe acute respiratory syndrome coronavirus 2 RNA on surfaces in quarantine rooms, Emerg. Infect. Dis. 26 (2020) 2162–2164.

[15] Centers for Disease Control and Prevention (CDC), Science brief: SARS-CoV-2 and surface (fomite) transmission for indoor community environments. https://www.cdc.gov/coronavirus/2019-ncov/more/science-and-research/surface-transmission.html, 2021. (Accessed 19 September 2021).

[16] Cable News Network (CNN), China has built a 5,000-room quarantine center for overseas arrivals. It could be the first of many. https://edition.cnn.com/2021/09/29/china/guangzhou-covid-quarantine-center-mic-intl-hnk/index.html, 2021. (Accessed 2 November 2021).

[17] A. Hoefer, D. Pampaka, E.R. Wagner, A.A. Herrera, E.G.R. Alonso, N. López-Perea, R.C. Portero, L. Herrera-León, S. Herrera-León, D.N. Gallo, Management of a COVID-19 outbreak in a hotel in Tenerife, Spain, Int. J. Infect. Dis. 96 (2020) 384–386.

[18] Centers for Disease Control and Prevention (CDC), Update: outbreak of severe acute respiratory syndrome - worldwide, 2003, MMWR (Morb. Mortal. Wkly. Rep.) 52 (12) (2003) 241–248.

[19] Q. Wang, Z. Lin, J. Niu, G.K.Y. Choi, J.C. Fung, A.K. Lau, Y. Li, Spread of SARS-CoV-2 aerosols via two connected drainage stacks in a high-rise housing outbreak of COVID-19, J. Hazard Mater. (2022), 128475.

[20] A. Bahadori-Jahromi, A. Rotimi, A. Mylona, P. Godfrey, D. Cook, Impact of window films on the overall energy consumption of existing UK hotel buildings, Sustainability 9 (5) (2017) 731–753.

[21] Confluence. https://confluence.cornell.edu/display/SIMULATION/FLUENT+-+Flow+over+an+Airfoil-+Step+6, 2021. (Accessed 8 January 2022).

[22] Y. Li, A. Delsante, J. Symons, Prediction of natural ventilation in buildings with large openings, Build. Environ. 35 (3) (2000) 191–206.

[23] Y. Li, S. Duan, I.T.S. Yu, T.W. Wong, Multi-zone modeling of probable SARS virus transmission by airflow between flats in Block E, Amoy Gardens, Indoor Air 15 (2) (2005) 96–111.

[24] S. Xiao, Y. Li, M. Sung, J. Wei, Z. Yang, A study of the probable transmission routes of MERS-CoV during the first hospital outbreak in the Republic of Korea, Indoor Air 28 (1) (2018) 51–63.

[25] M. Orme, M. Liddament, A. Wilson, Numerical Data for Air Infiltration and Natural Ventilation Calculations, International Energy Agency, Paris, 1998.

[26] T.L. Thatcher, A.C. Lai, R. Moreno-Jackson, R.G. Sextro, W.W. Nazaroff, Effects of room furnishings and air speed on particle deposition rates indoors, Atmos. Environ. 36 (11) (2002) 1811–1819.

[27] I.T. Yu, Y. Li, T.W. Wong, W. Tam, A.T. Chan, J.H. Lee, T. Ho, Evidence of airborne transmission of the severe acute respiratory syndrome virus, N. Engl. J. Med. 350 (17) (2004) 1731–1739.

[28] M.D. Hutton, W.W. Stead, G.M. Cauthen, A.B. Bloch, W.M. Ewing, Nosocomial transmission of tuberculosis associated with a draining abscess, JID (J. Infect. Dis.) 161 (2) (1990) 286–295.

[29] T.L. Gustafson, G.B. Lavely, E.R. Brawner Jr., R.H. Hutcheson Jr., P.F. Wright, W. Schaffner, An outbreak of airborne nosocomial varicella, Pediatrics 70 (4) (1982) 550–556.

[30] N. Wong, L. Cheng, E. Cheung, Coronavirus: what kind of lockdown can Hong Kong handle ... or is it even ready at all? South China Morning Post. https://www.scmp.com/news/hong-kong/health-environment/article/3168870/coronavirus-what-kind-lockdown-can-hong-kong, 2022. (Accessed 12 March 2022).

[31] G.D.W. McKendrick, R.T.D. Emond, Investigation of cross-infection in isolation wards of different design, Epidemiol. Infect. 76 (1) (1976) 23–31.

[32] J.D. Anderson, M. Bonner, D.W. Scheifele, B.C. Schneider, Lack of nosocomial spread of varicella in a pediatric hospital with negative pressure ventilated patient rooms, Infect. Control 6 (1985) 120–121, 03.

[33] Y. Sun, Z. Wang, Y. Zhang, J. Sundell, In China, students in crowded dormitories with a low ventilation rate have more common colds: evidence for airborne transmission, PLoS One 6 (11) (2011), e27140.

[34] J.O. Warner, J.A. Warner, The UK's hotel quarantine system is not fit for purpose, BMJ Opin. (2021). https://blogs.bmj.com/bmj/2021/06/04/the-uks-hotel-quarantine-system-is-not-fit-for-purpose/. (Accessed 2 November 2021).

[35] D. Slotta, Population distribution in Hong Kong 2020 by type of housing. https://www.statista.com/statistics/629802/hong-kong-population-by-type-of-housing/, 2021. (Accessed 13 January 2021).

[36] H. Lu, J. Li, X. Ni, Promoting resilience in the age of covid-19 pandemic: a new era of strategic foresight, Aging Dis. 12 (1) (2021) 1–2.

[37] J. Niu, T.C. Tung, On-site quantification of re-entry ratio of ventilation exhausts in multi-family residential buildings and implications, Indoor Air 18 (1) (2007) 12–26.

[38] D. Mu, N. Gao, T. Zhu, Wind tunnel tests of inter-flat pollutant transmission characteristics in a rectangular multi-storey residential building, part A: effect of wind direction, Build. Environ. 108 (2016) 159–170.

[39] D. Mu, C. Shu, N. Gao, T. Zhu, Wind tunnel tests of inter-flat pollutant transmission characteristics in a rectangular multi-storey residential building, part B: effect of source location, Build. Environ. 114 (2017) 281–292.

[40] D.J. Cui, C.M. Mak, J.L. Niu, Effect of balconies and upper-lower vents on ventilation and indoor air quality in a wind-induced, naturally ventilated building, Build. Serv. Eng. Technol. 35 (4) (2014) 393–407.

[41] Y. Wu, T.C. Tung, J.L. Niu, On-site measurement of tracer gas transmission between horizontal adjacent flats in residential building and cross-infection risk assessment, Build. Environ. 99 (2016) 13–21.

[42] Y. Wu, T.C. Tung, J.L. Niu, Experimental analysis of driving forces and impact factors of horizontal inter-unit airborne dispersion in a residential building, Build. Environ. 151 (2019) 88–96.

[43] K.R. Gautam, L. Rong, G. Zhang, M. Abkar, Comparison of analysis methods for wind-driven cross ventilation through large openings, Build. Environ. 154 (2019) 375–388.